INFECTION AND IMMUNITY, Oct. 2009, p. 4609–4620 Vol. 77, No. 10
0019-9567/09/$08.00+0 doi:10.1128/IAI.00301-09

Actin Dynamics and Rho GTPases Regulate the Size and Formation of Parasitophorous Vacuoles Containing *Coxiella burnetii*[▽]

Milton Aguilera, Romina Salinas, Eliana Rosales, Sergio Carminati, Maria I. Colombo, and Walter Berón*

Instituto de Histología y Embriología, Facultad de Ciencias Médicas, Universidad Nacional de Cuyo-CONICET, Mendoza 5500, Argentina

Received 16 March 2009/Returned for modification 16 April 2009/Accepted 16 July 2009

Q fever is a disease caused by *Coxiella burnetii*. In the host cell, this pathogen generates a large parasitophorous vacuole (PV) with lysosomal characteristics. Here we show that F-actin not only is recruited to but also is involved in the formation of the typical PV. Treatment of infected cells with F-actin-depolymerizing agents alters PV development. The small PVs formed in latrunculin B-treated cells were loaded with transferrin and Lysotracker and labeled with an antibody against cathepsin D, suggesting that latrunculin B did not affect vacuole cargo and its lysosomal characteristics. Nevertheless, the vacuoles were unable to fuse with latex bead phagosomes. It is known that actin dynamics are regulated by the Rho family GTPases. To assess the role of these GTPases in PV formation, infected cells were transfected with pEGFP expressing wild-type and mutant Rac1, Cdc42, and RhoA proteins. Rac1 did not show significant PV association. In contrast, PVs were decorated by both the wild types and constitutively active mutants of Cdc42 and RhoA. This association was inhibited by treatment of infected cells with chloramphenicol, suggesting a role for bacterial protein synthesis in the recruitment of these proteins. Interestingly, a decrease in vacuole size was observed in cells expressing dominant-negative RhoA; however, these small vacuoles accumulated transferrin, Lysotracker, and DQ-BSA. In summary, these results suggest that actin, likely modulated by the GTPases RhoA and Cdc42 and by bacterial proteins, is involved in the formation of the typical PV.

Coxiella burnetii, the causative agent of human Q fever, is an obligate intracellular bacterium which is found in a wide range of hosts, including livestock and humans. In the case of humans, the primary route of infection is via the inhalation of contaminated aerosols (65). In infected animals, *C. burnetii* organisms are excreted in milk, urine, and feces, and the bacteria are dispersed together with the amniotic fluids and the placenta during animal birthing. These bacteria can survive long periods in the environment, since they are highly resistant to heat, drying, and common disinfectants. *C. burnetii* inhabits mainly monocytes/macrophages but can infect a wide variety of host cells in vitro (5). This bacterium resides in an acidic parasitophorous vacuole (PV) with late endosome-lysosome characteristics (7, 25, 27, 55). It was recently shown that the PV also interacts with the autophagic pathway, acquiring autophagosomal features (7, 24, 55).

Phagocytosis is the process by which professional and nonprofessional phagocytes ingest microbes, cell debris, apoptotic cells, and other large particles (52). Particle internalization involves activation of several signaling pathways that orchestrate remodeling of the actin cytoskeleton, plasma membrane extension, particle engulfment, and phagosome formation (45, 56, 61). Proteins present in the phagosome provide the molecular machinery required for numerous functions within the cell that are dependent on phagosome maturation, such as the killing of internalized pathogens. Phagosome maturation involves a series of fission and fusion events with endosomes and lysosomes. Thus, the resulting phagolysosome is highly hydrolytic and limits pathogen replication (26, 66).

Most cells undergo rapid remodeling of the actin cytoskeleton to regulate cellular processes such as adhesion (15), motility (41), apoptosis (21), and vesicle transport (53, 59). These events are driven by numerous actin-associated proteins and several upstream signaling molecules. The coordinated activities of these factors control with exquisite precision the spatial and temporal assembly of actin structures and ensure the dynamic turnover of the actin architecture such that cells can rapidly alter their cytoskeleton in response to internal and external signals.

Rho family proteins are monomeric GTPases that regulate a wide range of cellular activities, such as the cell cycle, morphogenesis, gene transcription, and cell movement (32). Some of them are tightly associated with the actin cytoskeleton. The best-characterized members of the Rho family are Rho, Rac, and Cdc42, and each one regulates a different type of actin-based structure. Rho and Rac are involved in the formation of stress fibers and lamellipodia, respectively, while Cdc42 plays an important role in the formation of filipodia (4, 38). More recently, Rho proteins and actin have been shown to participate in the secretory pathway. Cdc42, together with ARF1, coatomer, actin, and actin-binding proteins, is an important molecular component in endoplasmic reticulum-Golgi transport (11, 18, 44). There is increasing evidence connecting endocytosis, Rho proteins, and the actin cytoskeleton. Macropinocytosis and clathrin-dependent and -independent endocytosis are processes that require diverse Rho

* Corresponding author. Mailing address: Instituto de Histología y Embriología (IHEM)-CONICET, Facultad de Ciencias Médicas, Universidad Nacional de Cuyo Casilla de Correo 56, Centro Universitario, Parque General San Martín, 5500 Mendoza, Argentina. Phone: 54-261-4135000, ext. 2641. Fax: 54-261-4494117. E-mail: wberon@fcm.uncu.edu.ar.

▽ Published ahead of print on 27 July 2009.

GTPases (51). Multiple actin cytoskeleton regulators, such as Abp1, cortactin, profilin, and Hip, can interact with endocytic proteins, such as clathrin, AP2, and dynamin, suggesting a connection between actin dynamics and endocytosis (35, 47).

In phagocytosis, Rho proteins also control the actin cytoskeleton rearrangements needed for particle internalization by phagocytes (50). Fcγ- and complement receptor-mediated phagocytosis, also called type I and type II phagocytosis, respectively, has been described for macrophages. In type I phagocytosis, the Fcγ-opsonized particles are engulfed by the extension of pseudopods that subsequently fuse to form the phagosome. In type II phagocytosis, particles opsonized with complement sink into a phagocytic cup and are internalized without pseudopod formation. In these processes, different signaling pathways are activated. Rac/Cdc42 and Rho, along with their specific effectors, are activated during type I and type II phagocytosis, respectively (10). As mentioned before, actin filaments (F-actin) regulate several processes related to plasma membrane function but also processes such as motility and fusion of endosomes, lysosomes, and phagosomes (33, 36, 60, 68). Interestingly, actin filaments accumulate around phagosomes harboring *Salmonella* (62), *Leishmania* (40, 42), and nonpathogenic or pathogenic mycobacteria (22, 23), suggesting that actin recruitment may participate in the intracellular survival of these pathogens.

In this report, we investigate the relationship between the actin cytoskeleton and the intracellular trafficking of *C. burnetii*. We show that PVs recruit F-actin and that F-actin disassembly significantly inhibits the formation of these vacuoles. Additionally, Cdc42 and RhoA, but not Rac1, were able to interact with the PV, in a bacterial protein synthesis-dependent manner. Our results imply that F-actin, Cdc42, and RhoA are involved in the formation of the typical PV.

MATERIALS AND METHODS

Materials. Dulbecco's modified Eagle medium (DMEM), fetal bovine serum, penicillin, and streptomycin were obtained from Gibco BRL/Life Technologies (Buenos Aires, Argentina). Plasmids encoding enhanced green fluorescent protein (EGFP)-Rac1, -Cdc42, and -RhoA and their mutants were kindly provided by Philippe Chavrier (Centre National de la Recherche Scientifique/Institut Curie, Paris, France) and Mark R. Phillips (Laboratory of Molecular Rheumatology, NYU School of Medicine). The rabbit polyclonal anti-*Coxiella* antibody was generously provided by Robert Heinzen (Rocky Mountain Laboratories, NIAID, NIH, Hamilton, MT).

Rhodamine- or fluorescein isothiocyanate (FITC)-conjugated phalloidin and anti-rabbit antibodies were obtained from Sigma Chemical Co. (Buenos Aires, Argentina). The DNA marker Hoechst 33342, Lysotracker, and DQ-BSA (a modified bovine serum albumin [BSA] that is cleaved and becomes fluorescent when it reaches hydrolytic compartments) were purchased from Molecular Probes (Eugene, OR). Secondary antibodies were purchased from Jackson ImmunoResearch Laboratories, Inc. (West Grove, PA). Polybead polystyrene microspheres (3 μm) were purchased from Polyscience, Inc. (Warrington, PA). All other chemicals were from Sigma Chemical Co. (Buenos Aires, Argentina). Latrunculin B and cytochalasin D were stored at −20°C as 20 mM stock solutions in dimethyl sulfoxide (DMSO).

Cell culture. HeLa cells were grown in DMEM supplemented with 10% heat-inactivated fetal bovine serum, 2.2 g/liter sodium bicarbonate, 2 mM glutamine, and 0.1% penicillin-streptomycin at 37°C under 5% CO_2.

Propagation of *Coxiella burnetii* phase II cells. *C. burnetii* clone 4, phase II, strain Nine Mile bacteria, which are infective for cultured cells but not for mammals, were provided by Ted Hackstadt (Rocky Mountain Laboratories, NIAID, NIH, Hamilton, MT) and handled in a biosafety level II facility. Nonconfluent Vero cells were cultured in T25 flasks at 37°C under 5% CO_2 in DMEM supplemented with 5% fetal bovine serum, 0.22 g/liter sodium bicarbonate, and 20 mM HEPES, pH 7 (MfbH). Cultures were infected with *C. burnetii* phase II suspensions for 6 days at 37°C under 5% CO_2. After being frozen at −70°C, the flasks were thawed and the cells scraped and passed 20 times through a 27-gauge needle connected to a syringe. Cell lysates were centrifuged at 800 × *g* for 10 min at 4°C. The supernatants were centrifuged at 24,000 × *g* for 30 min at 4°C, and pellets containing *C. burnetii* were resuspended in phosphate-buffered saline (PBS), aliquoted, and frozen at −70°C.

Infection of HeLa cells with *Coxiella burnetii*. A total of 5×10^5 cells were seeded on sterile glass coverslips placed in 24-well plates and grown overnight in MfbH. For infection, a 5-μl aliquot of *C. burnetii* suspension was added to each well (multiplicity of infection, approximately 20). Cells were incubated overnight (16 h) at 37°C under 5% CO_2.

Fluorescence staining. HeLa cells were fixed with 2% paraformaldehyde solution in PBS for 10 min at 37°C, washed with PBS, and blocked with 50 mM NH_4Cl in PBS. Subsequently, cells were permeabilized with 0.05% saponin in PBS containing 0.5% BSA and then incubated with primary antibodies against *C. burnetii* (1:800) and cathepsin D (1/50). After being washed, cells were incubated with secondary antibodies conjugated with rhodamine, FITC, or Cy5 (1:200). To detect F-actin, rhodamine- or FITC-conjugated phalloidin was used. Cells were mounted with Mowiol and examined by fluorescence microscopy.

Treatment of infected cells with F-actin-depolymerizing agents. After overnight infection, cells were washed with PBS and incubated at 37°C under 5% CO_2 for 32 h with MfbH containing 0.05% DMSO, 10 μM latrunculin B, or cytochalasin D. Treated cells were either fixed and processed by fluorescence microscopy or washed, reincubated for 24 h in the absence of the drugs, and then processed as indicated above.

Cell transfection. Infected cells were transfected for 8 h with 2 μg/ml empty pEGFP vector or pEGFP encoding RhoA, Cdc42, or Rac1, using the Lipofectamine 2000 reagent (Invitrogen, Buenos Aires, Argentina) according to the manufacturer's instructions. Transfected cells were incubated for 40 h at 37°C under 5% CO_2 in MfbH.

Chloramphenicol treatment of infected cells. *C. burnetii*-infected cells were transfected for 8 h with pEGFP encoding wild-type Cdc42 (Cdc42 WT) or RhoA WT as described above. After transfection, the cells were washed several times and incubated for 24 h at 37°C under 5% CO_2, with or without 50 μg/ml chloramphenicol. Cells were fixed and processed for fluorescence microscopy as indicated above.

Assays to determine cargo and lysosomal characteristics of *C. burnetii*-containing vacuoles. Transfected or untransfected infected cells were incubated with either 1 μM Lysotracker or 10 μg/ml DQ-BSA for 2 h at 37°C or with 10 μg/ml Alexa 633-transferrin (Molecular Probes, Inc.) for 1 h at 37°C. After several washes, the cells were fixed and processed for indirect immunofluorescence.

Latex bead uptake assay. Latex beads (500 μl of a 5% suspension) were coated with 50 μg/ml rhodamine overnight at 4°C with gentle shaking. After being washed three times with PBS, the beads were incubated with 25 μg/ml mouse anti-myc monoclonal antibody (Sigma Chemical Co., Buenos Aires, Argentina) overnight at 4°C with gentle shaking. The beads were washed three times with PBS and resuspended in 500 μl MfbH. HeLa cells were plated on coverslips distributed in 24-well plates (2.5×10^4 cells/well) and incubated for 6 h at 37°C under 5% CO_2. The cells were infected with 5 μl *C. burnetii* suspension per well and incubated overnight at 37°C under 5% CO_2. After several washes with PBS, cells were incubated in MfbH with 5 μl of coated latex bead suspension per well for 3 h at 37°C under 5% CO_2. Cells were washed three times with PBS and incubated for 45 h at 37°C under 5% CO_2 in MfbH containing 0.1% DMSO or 10 μg/ml latrunculin B. The cells were fixed as mentioned above and incubated with a FITC-conjugated goat anti-mouse antibody in the absence of detergent to detect the extracellular beads. The cells were then incubated sequentially with rabbit anti-*C. burnetii* antibody and Cy5-conjugated donkey anti-rabbit in the presence of detergent to estimate the total number of beads. The samples were analyzed with an FV1000 Olympus confocal microscope.

Determination of size distribution of *C. burnetii*-containing vacuoles. About 30 cells per coverslip (in triplicate) were scored to determine the area of the *C. burnetii*-containing vacuoles, using a Nikon Eclipse 2000 microscope with a ×60 objective. Infected cells were defined as those with at least one bacterium inside, detected by immunofluorescence. The sizes of the vacuoles were determined by morphometric analysis, using ImageJ software. Vacuole sizes were grouped into two categories, namely, small vacuoles (smaller than 22 μm^2) and large vacuoles (larger than 22 μm^2).

Fluorescence microscopy. HeLa cells were analyzed by fluorescence microscopy using an inverted microscope (Nikon Eclipse 2000; Nikon, Japan). Images were obtained with a charge-coupled device camera (Orca I; Hamamatsu) and processed using the Metamorph program, series 6.1 (Universal Images Corporation). Confocal images were obtained with a Nikon C1 confocal microscope system and with the EZ-C1 program (Nikon, Japan) or with an Olympus FV1000

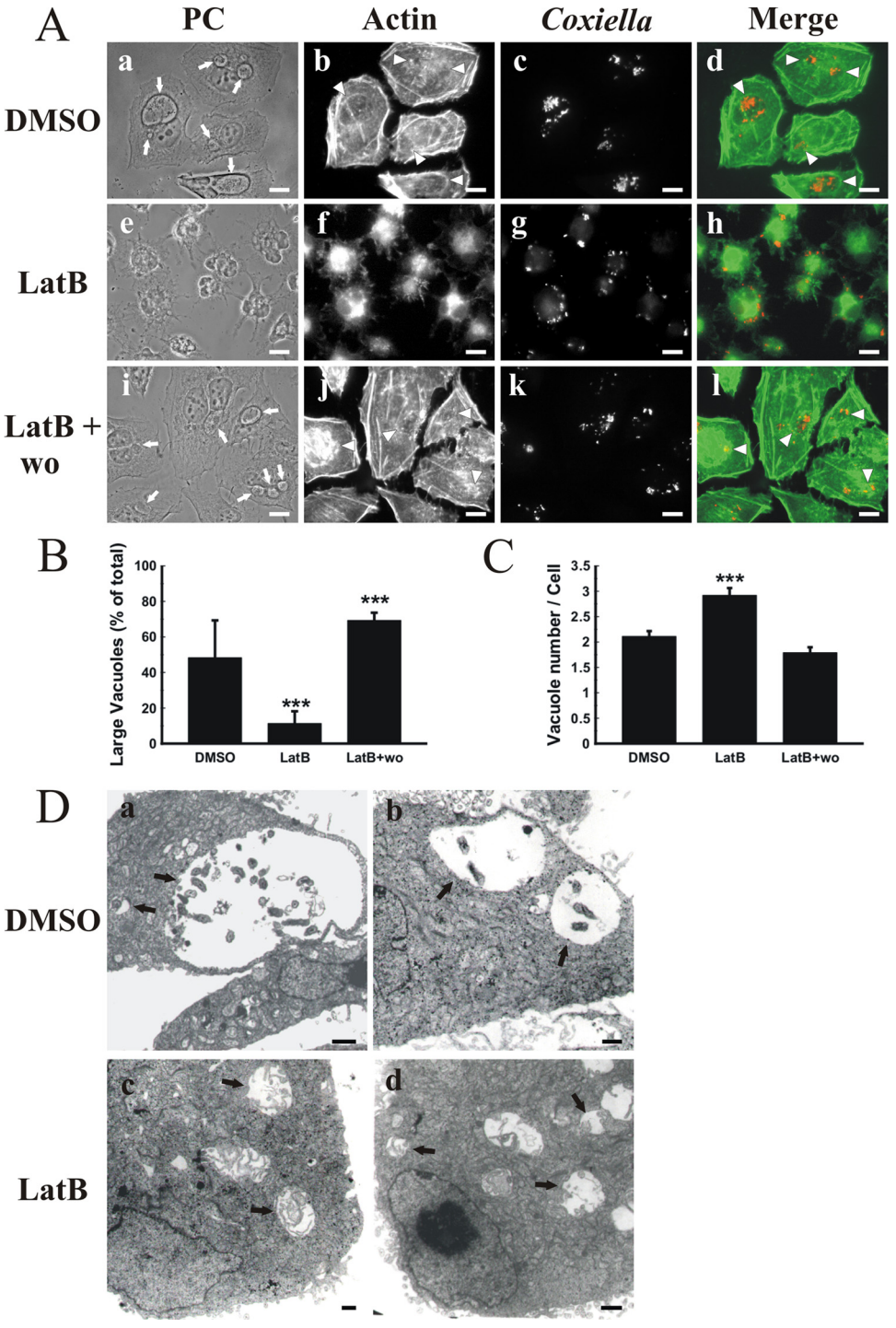

FIG. 1. F-actin associates with and regulates the formation of PVs. (A) F-actin is recruited to the PV. HeLa cells infected for 16 h with *C. burnetii* were incubated for 32 h with 0.05% DMSO (control) (a to d) or 10 μM latrunculin B (LatB) (e to h). After latrunculin incubation, cells were washed and incubated for 24 h with fresh medium without latrunculin (LatB + wo) (i to l). After cell fixation, F-actin and *C. burnetii* were stained with rhodamine-phalloidin (green) (b, f, and j) and a specific anti-*C. burnetii* antibody (red) (c, g, and k), respectively. Cells were analyzed by phase-contrast (PC) (a, e, and i) and fluorescence (b, c, f, g, j, and k) microscopy. Micrographs of representative cells are shown. PVs are indicated by arrows. The colocalization between PVs and F-actin is shown in the merge column (d, h, and l). Either small F-actin patches or F-actin rings surrounding PVs are indicated by arrowheads. Bars, 15 μm. (B) F-actin disassembly reduces PV size. Cells were treated and processed as described for panel A. The sizes of the vacuoles were determined by morphometric analysis using the ImageJ program. Large vacuoles correspond to the PV population of ≥22 μm^2. Results are expressed as means ± standard errors (SE) for at least three independent experiments. ***, $P < 0.001$. (C) F-actin disassembly increases the number of PVs. Cells were treated and processed as described for panel A, and the number of vacuoles per cell was determined by morphometric analysis with ImageJ software (see Materials and Methods). Results are expressed as means ± SE for at least three independent experiments. ***, $P < 0.001$. (D) Analysis of infected cells by transmission electron microscopy. HeLa cells infected for 16 h with *C. burnetii* were incubated for 32 h with 0.05% DMSO (control) (a and b) or 10 μM latrunculin B (LatB) (c and d) and then processed for transmission electron microscopy using conventional techniques. Electron micrographs of representative cells are shown. PVs are indicated by arrows. Bars, 1 μm.

confocal microscope and the FV 10-ASW 1.7 program (Olympus, Japan). Images were processed using ImageJ software (NIH [http://rsb.info.nih.gov/ij]). Normally, when a protein associates with the PV limiting membrane, the EGFP-tagged protein is visualized as a ring surrounding luminal bacteria; hence, there is no superposition of the green and red channels. Therefore, colocalization was considered to be positive when, after drawing of a line across the PV, the fluorescent label of the bacterium was located between two peaks of EGFP.

Transmission electron microscopy. Cells were fixed with 2% glutaraldehyde in PBS. After 10 min, the samples were centrifuged for 15 min at 12,000 × *g*, and the pellets were processed for transmission electron microscopy using conventional techniques.

Statistical analysis. The data were analyzed by the Kolmogorov-Smirnov nonparametric test and by analysis of variance in conjunction with Tukey and Dunnett tests.

RESULTS

F-actin associates with the prototypical PV and modulates its formation. It is known that F-actin plays an important role in different vesicular transport processes (53). Moreover, F-actin is involved in the fusion of phagosomes with endocytic compartments (33, 36, 60). The formation of the large PV is a result of homotypic fusion among small phagosomes containing *C. burnetii* (20, 25, 28, 63). To assess whether F-actin is involved in PV formation, HeLa cells were infected for 16 h at 37°C, and after being washed to remove noninternalized bacteria, the cells were incubated for 32 h with the F-actin-depolymerizing toxins latrunculin B and cytochalasin D or with vehicle. Cells were fixed, processed for indirect immunofluorescence, and analyzed by fluorescence microscopy. F-actin was detected with FITC-phalloidin, and *C. burnetii* was detected with a specific antibody. At 32 h postinfection, *C. burnetii* usually forms a large PV that may even displace the nucleus from the cell center. Additionally, some smaller vesicles containing bacteria are visualized (Fig. 1A, panel a). In control cells, F-actin was observed around the PV in small patches, and an F-actin ring was also observed, although less frequently (Fig. 1A, panels b and d). In latrunculin-treated cells, the F-actin was depolymerized and the soluble actin dispersed throughout the cytoplasm, with an altered cell shape. Small but not large PVs were observed (panels e, g, and h). This phenomenon was reversible since the large PVs reappeared when the drugs were washed out and incubation was prolonged for an additional 24 h (panels i to l). A similar, although less pronounced, effect was observed in cells treated with cytochalasin D (data not shown).

Because PV size is usually heterogeneous (from small vacuoles to the typical large PVs), we defined two categories, small and large vacuoles (smaller and larger than 22 μm^2, respectively), by using Image J software to determine if the treatment modified the size of the vacuoles. As shown in Fig. 1B, approximately 50% of the PVs were large (i.e., larger than 22 μm^2). In latrunculin-treated cells, a marked reduction in the population of large PVs was observed, as only 12% of the PVs were larger than 22 μm^2. When the drug was removed and incubation in fresh medium was continued, the size of the vacuoles was recovered. When the number of PVs was analyzed, a significant increase was observed in latrunculin-treated cells compared to controls. When the drug was washed out, the number of vacuoles returned to the value observed in control cells (Fig. 1C). These results were corroborated by transmission electron microscopy (Fig. 1D). Consistent with the confocal images, latrunculin-treated cells showed numerous PVs of smaller size (Fig. 1D, panels c and d), while untreated cells presented a small number of vacuoles of the larger size (panels a and b).

Taken together, these results suggest that F-actin not only is recruited to the PV membrane but also is involved in the biogenesis of the large compartment containing *C. burnetii*.

F-actin regulates fusion between PVs and bead-containing phagosomes. It is possible that actin dynamics modulate the functional properties of the PV, such as the well-reported fusogenic activity with endocytic and phagocytic compartments (20, 25, 28, 63). To test this hypothesis, infected HeLa cells were incubated with transferrin or latex beads, as an endocytic or phagocytic probe, respectively, and then the coalescence of the probes and *C. burnetii* in the same vacuole was estimated. Most *Coxiella*-containing vacuoles, in control as well as in latrunculin-treated cells, were loaded with transferrin (Fig. 2A). On the other hand, as shown in Fig. 2B and C, latrunculin significantly inhibited the colocalization of the phagocytic probe with the bacteria (21% versus 72%). These results suggest that F-actin plays a role in the fusion of vacuoles containing *C. burnetii* with latex bead-containing phagosomes. In contrast, the lack of polymerized actin did not seem to substantially affect the interaction with other endocytic compartments.

F-actin regulates the formation of the PV without affecting its maturation. We observed that in cells infected for 16 h and then treated for 32 h with latrunculin, *Coxiella*-containing vacuoles were labeled with the endosomal marker transferrin and with Lysotracker, a marker of acidic compartments (data not shown). These results suggest that *C. burnetii* transits along the endophagosomal pathway to finally arrive at an acidic phagolysosomal compartment. It has been reported that PV maturation to a phagolysosome takes approximately 2 h (1, 27, 64). To analyze if latrunculin has an effect on PV maturation, HeLa cells were infected for 1 h and then treated with latrunculin for 47 h. The cells were either fixed to analyze the presence of the lysosomal enzyme cathepsin D by indirect immunofluorescence or incubated for 1 h with Lysotracker before fixation. As shown in Fig. 3A and B, vacuoles containing *C. burnetii* were labeled with both markers. These results suggest that latrunculin treatment did not modify the maturation of the vacuoles.

Rho proteins are recruited to the PV membrane. GTPases of the Rho family function as important regulators of actin dynamics (4, 9). To examine the role of these GTPases in PV formation, HeLa cells infected for 16 h with *C. burnetii* were transfected with pEGFP vectors encoding WT Cdc42, RhoA, or Rac1. As shown in Fig. 4A, EGFP-Cdc42 WT (panel d) and EGFP-RhoA WT (panel g) localized to filipodia and lamellipodia, respectively. Interestingly, the PV membrane recruited both proteins (panels f and i). In contrast, while EGFP-Rac1 WT localized to the cell cortex (panel j), it did not show any significant association with the PV (panel l). When the PV-protein colocalization was quantified (Fig. 4B), a highly significant colocalization with the PV (around 80%) was observed for both EGFP-Cdc42 and EGFP-RhoA compared with EFGP (control). Interestingly, treating cells with latrunculin B did not affect the recruitment of RhoA and Cdc42 WT to the PV membrane (data not shown). These results suggest that the association of the Rho GTPases occurs prior to the actin-dependent processes that maintain vacuole size and shape.

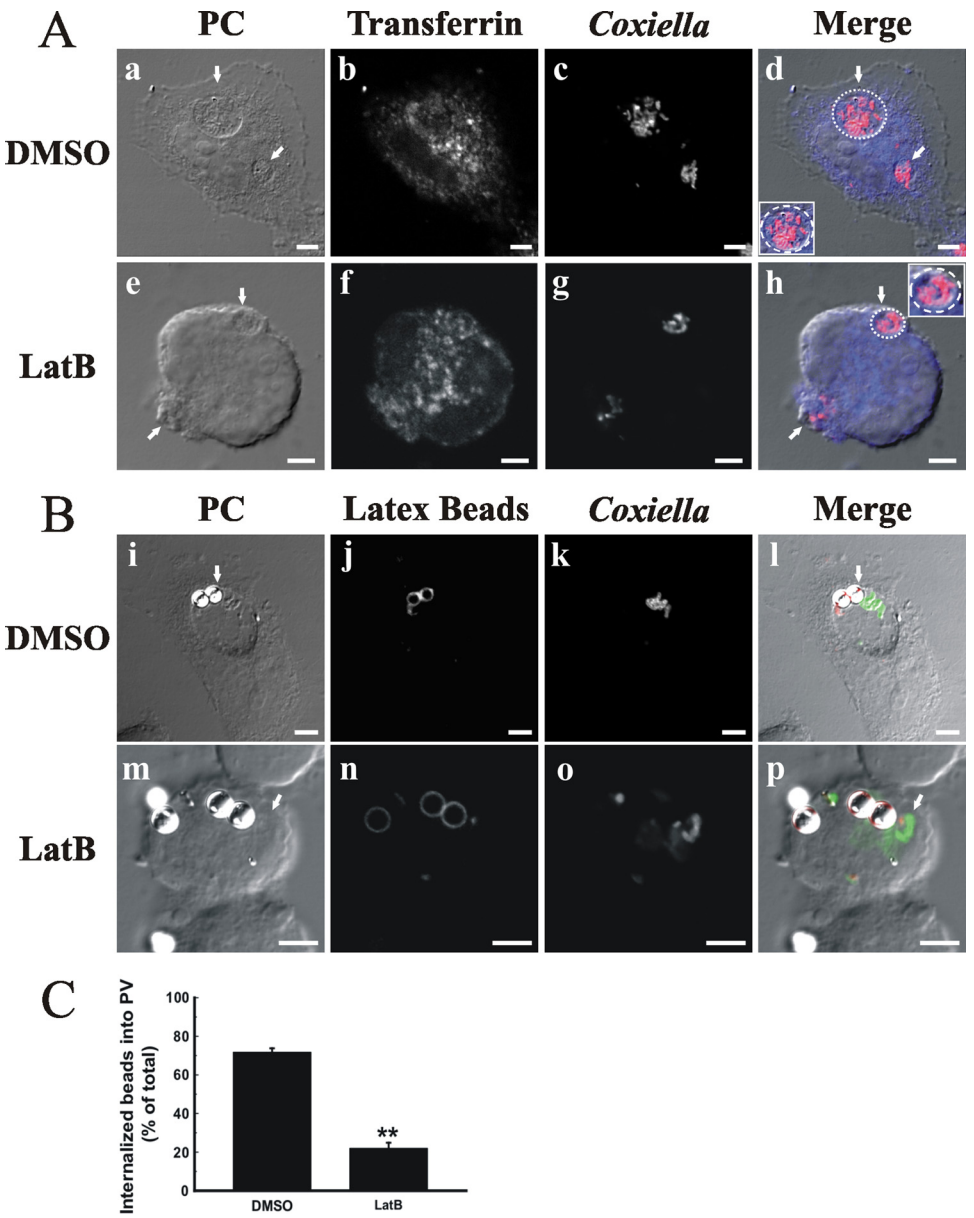

FIG. 2. F-actin is required for fusion between PVs and bead-containing phagosomes. Infected cells were incubated with either transferrin (A) (blue; b and f) or latex beads (B) (red; j and n) (see Materials and Methods) and treated as indicated in the legend to Fig. 1. *C. burnetii* cells were stained with a specific antibody (red [c and g] or green [k and o]). Cells were analyzed by phase-contrast (PC) (a, e, i, and m) and fluorescence (b, c, f, g, j, k, n, and o) microscopy. Colocalization of the different probes with the PVs is shown in the merge column (d, h, l, and p) and quantified in panel C. Micrographs of representative cells are shown. PVs are indicated by arrows. Insets in panels d and h show the localization of transferrin (blue) in the delineated vacuoles harboring the bacteria (red). Results are expressed as means ± SE for at least three independent experiments. **, $P < 0.01$. Bars, 5 μm.

It has been shown that *C. burnetii* protein synthesis regulates PV biogenesis (29). If the recruitment of Rho proteins to the vacuole is mediated by *C. burnetii*, then the proteins will not associate with the vacuole limiting membrane in transfected cells treated with chloramphenicol. As shown in Fig. 4C and D, chloramphenicol treatment significantly diminished the recruitment of both EGFP-Cdc42 and -RhoA compared to that in untreated cells. These results suggest that bacterial protein synthesis is required for the association of Rho proteins with the PV.

It is known that these Rho GTPases cycle between the GTP-bound, active form and the GDP-bound, inactive form. The GDP/GTP cycling of Rho family proteins is controlled mainly by the following three distinct functional classes of regulatory proteins: guanine nucleotide exchange factors, guanine nucleotide dissociation inhibitors, and GTPase-activating proteins (GAPs). These regulators control membrane association and binding and the hydrolysis of bound nucleotides (9). To determine whether the association of Rho proteins with the PV depends on their nucleotide binding state, cells were transfected with plasmids en-

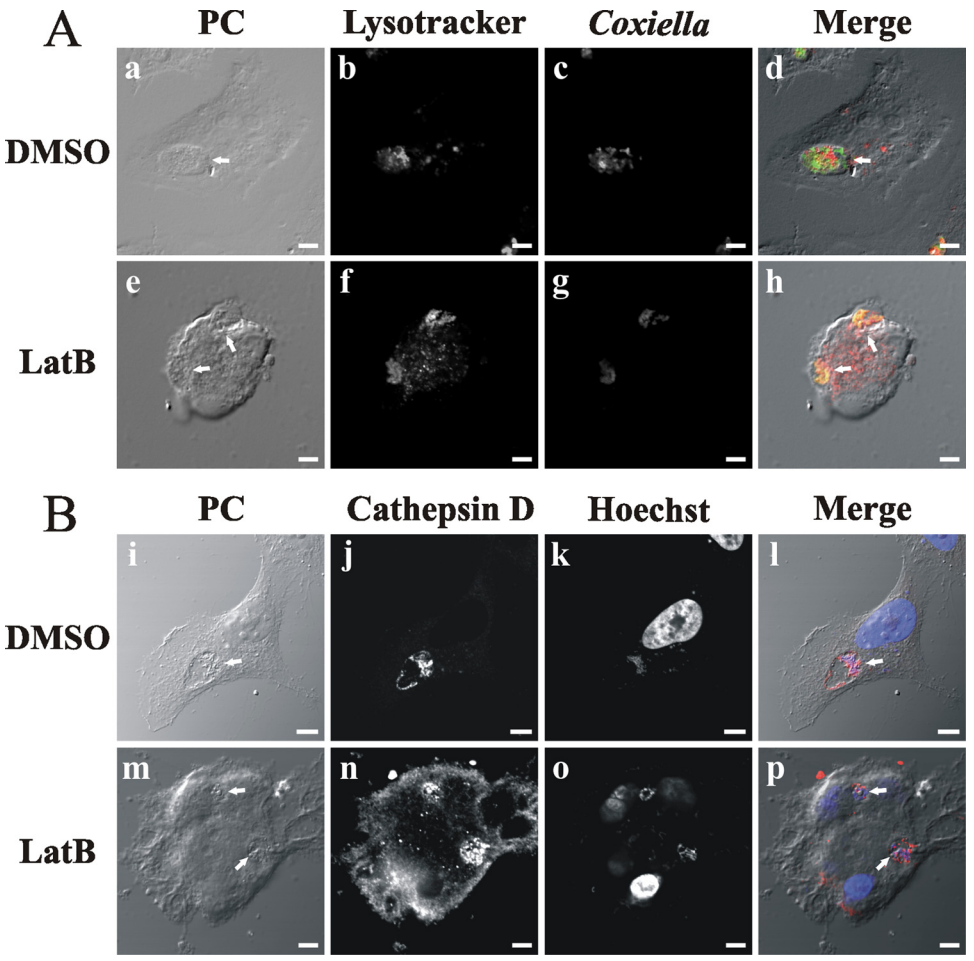

FIG. 3. F-actin regulates the formation of the PV without affecting its lysosomal characteristics. HeLa cells were infected for 1 h with *C. burnetii* and then incubated for 47 h with 0.05% DMSO (A [a to d] and B [i to l]) or 10 μM latrunculin B (LatB) (A [e to h] and B [m to p]). The cells were either incubated with Lysotracker (red) (b and f), a marker of acidic compartments, before fixation (A) or fixed to analyze the presence of the lysosomal enzyme cathepsin D (B). After fixation, cells were labeled with an anti-cathepsin D antibody (red) (B [j and n]), anti-*C. burnetii* (green) (A [c and g]), or Hoechst dye (blue) (B [k and o]). Cells were analyzed by phase-contrast (PC) (a, e, i, and m) and fluorescence (b, c, f, g, j, k, n, and o) microscopy. Micrographs of representative cells are shown. PVs are indicated by arrows. The colocalization between PVs and Lysotracker or cathepsin D is shown in the merge column (d, h, l, and p). Bars, 5 μm.

coding constitutively active or dominant-negative GTPases. In cells transfected with the constitutively active mutants pEGFP-Cdc42 V12 and -RhoA V14, practically 80% of PVs were labeled by these expressed proteins (Fig. 5A and B), whereas the constitutively active mutant EGFP-Rac1 V12 did not show any significant association with the PV (Fig. 5B).

To test whether Rho protein recruitment to the PV membrane is accompanied by F-actin, infected HeLa cells were transfected with constitutively active mutants of either Cdc42 or RhoA and then incubated with rhodamine-conjugated phalloidin to detect F-actin. The constitutively active mutants of either Cdc42 (Fig. 5C, panels a to h) or RhoA (panels i to p) colocalized with F-actin at the PV membrane. In contrast, as shown in Fig. 6A and B, the dominant-negative mutants of Cdc42, RhoA, and Rac1 did not significantly localize to the PV membrane compared with the case in control cells expressing EGFP alone. These results indicate that, as expected, it is mainly the GTP-bound form of the Rho proteins which is recruited to the PVs.

Overexpression of the dominant-negative mutant RhoA N19 affects PV size without modifying its cargo and lysosomal characteristics. We noticed that among all tested proteins, the overexpression of EGFP-RhoA N19 caused the most striking PV size changes, similar to latrunculin treatment. Therefore, we next analyzed in more detail the effect of the overexpression of RhoA N19 on vacuole size distribution. As indicated in Fig. 6C, a highly significant decrease in the population of vacuoles larger than 22 μm^2 was observed in cells expressing EGFP-RhoA N19 versus EGFP (16.6 and 45.5%, respectively), while the expression of either EGFP-Cdc42 N17 or EFGP-Rac1 N17 did not significantly affect the vacuole size distribution (50 and 51%, respectively). It is possible that the change in PV size distribution in cells overexpressing EGFP-RhoA N19 could be related to alterations in PV cargo and lysosomal characteristics (i.e., fusion with endosomal/lysosomal compartments). To test this hypothesis, infected HeLa cells were transfected with either pEGFP or pEGFP-RhoA N19 and then incubated with Lysotracker, Alexa 633-transferrin, or DQ-BSA. As mentioned before, Lysotracker and transferrin label

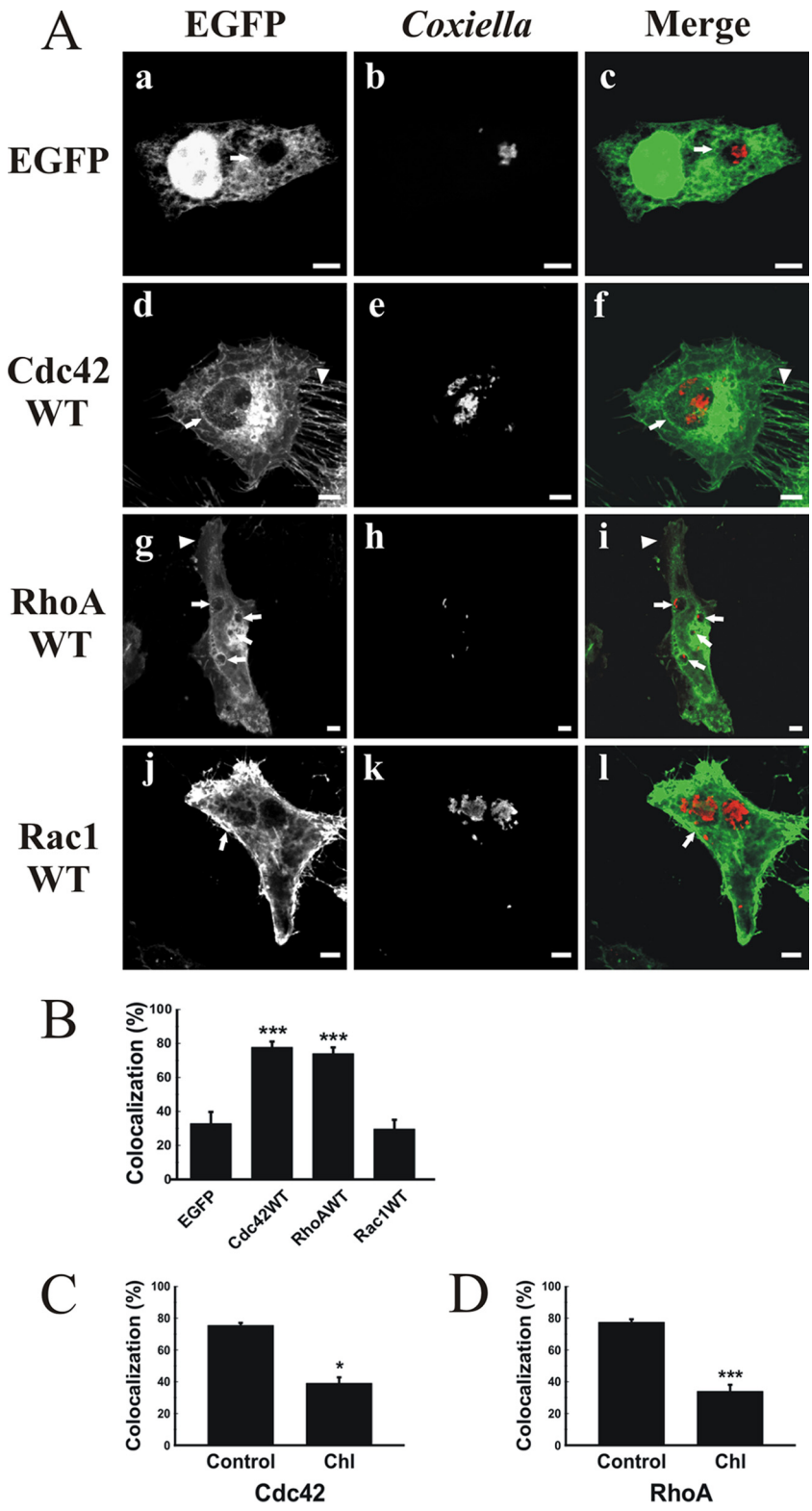

FIG. 4. PVs are decorated with the WT forms of EGFP-Cdc42 and -RhoA but not with EGFP-Rac1. (A) HeLa cells were infected as indicated in the legend to Fig. 1 and then transfected with pEGFP alone (a to c), pEGFP-Cdc42 WT (d to f), pEGFP-RhoA WT (g to i), or pEGFP-Rac1 WT (j to l) as described in Materials and Methods. After 24 h, cells were fixed and processed for immunofluorescence, using a specific anti-*C. burnetii* antibody (red) (b, e, h, and k). Cells were analyzed by confocal microscopy. Micrographs of representative cells are shown. PVs are indicated by arrows. Filipodia (d) and lamellipodia (g) are indicated by arrowheads. The colocalization between PVs and overexpressed proteins is shown in the merge column (c, f, i, and l). Bars, 5 μm. (B) Quantification of colocalization between PVs and EGFP fusion proteins. Results are expressed as means ± SE for at least three independent experiments. ***, $P < 0.001$. (C and D) Chloramphenicol treatment reduces the colocalization of PVs with EGFP-Cdc42 and EGFP-RhoA. Infected cells were transfected with pEGFP-Cdc42 WT (C) or pEGFP-RhoA WT (D) and then treated with chloramphenicol (Chl) as indicated in Materials and Methods. Colocalization between PVs and EGFP fusion proteins was quantified. Results are expressed as means ± SE for at least three independent experiments. *, $P < 0.05$; ***, $P < 0.001$.

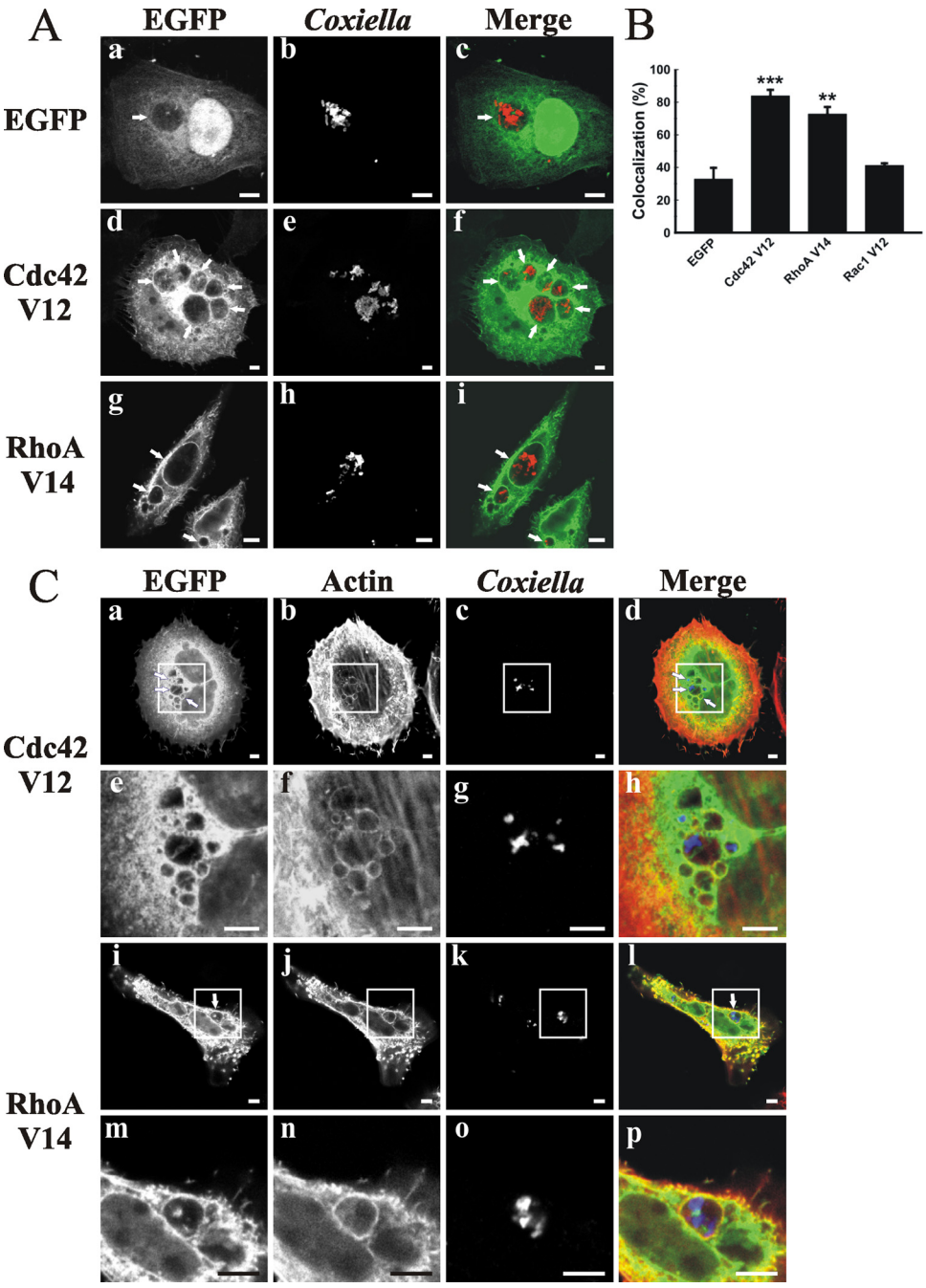

FIG. 5. EGFP-Cdc42 V12, EGFP-RhoA V14, and F-actin are recruited to the PV. (A) EGFP-Cdc42 V12 and -RhoA V14, but not EGFP-Rac1 V12, associated with PVs. HeLa cells were infected with *C. burnetii* and then transfected with pEGFP (a to c), pEGFP-Cdc42 V12 (d to f), or pEGFP-RhoA V14 (g to i). After 24 h, the cells were fixed and processed for immunofluorescence, using a specific anti-*C. burnetii* antibody (red) (b, e, and h). Cells were analyzed by confocal microscopy. Micrographs of representative cells are depicted. PVs are indicated by arrows. The colocalization is shown in the merge column (c, f, and i). (B) Quantification of colocalization. Results are expressed as means ± SE for at least three independent experiments. **, $P < 0.01$; ***, $P < 0.001$. (C) EGFP-Cdc42 V12, EGFP-RhoA V14, and F-actin colocalize with PVs. Infected HeLa cells were transfected with pEGFP-Cdc42 V12 (a to d) or pEGFP-RhoA V14 (i to l). After 24 h, cells were fixed and processed for immunofluorescence, using phalloidin-rhodamine to label actin (red) (b and j) and a specific anti-*C. burnetii* antibody (blue) (c and k). Panels e to h and m to p represent a magnification of the insets. Cells were analyzed by confocal microscopy. Micrographs of representative cells are depicted. PVs are indicated by arrows. The colocalization is shown in the merge column (d, h, l, and p). Bars, 5 μm.

acidic and endocytic compartments, respectively, and DQ-BSA is a modified BSA that is cleaved and becomes fluorescent when it reaches hydrolytic compartments, such as the lysosomes. As shown in Fig. 7, most PVs formed in transfected cells presented acidic (Lysotracker positive) (panel f) and hydrolytic (degraded DQ-BSA) (panel b) characteristics and also accumulated endocytosed transferrin (panel j). Similar results were obtained with untransfected cells (data not

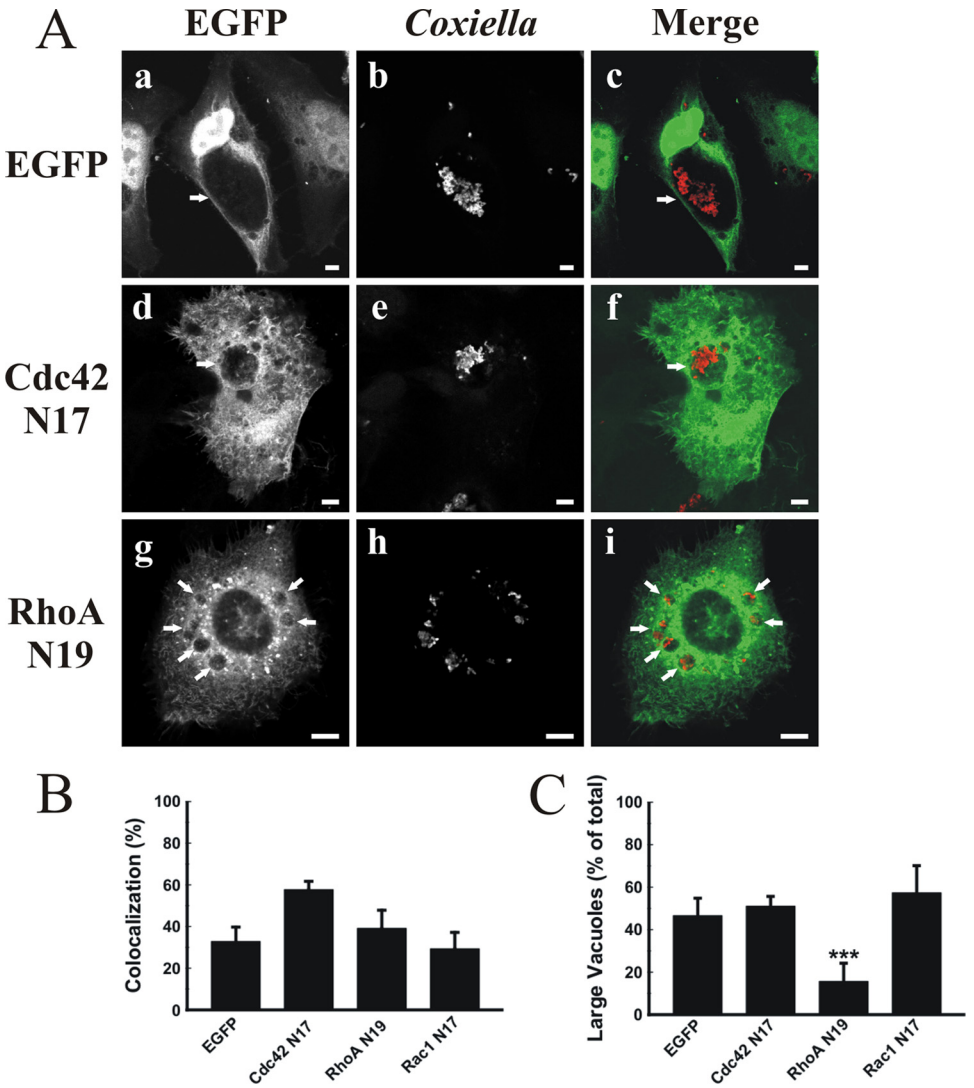

FIG. 6. The dominant-negative mutants of Cdc42, RhoA, and Rac1 are not recruited to the PV. (A) Infected HeLa cells were transfected with pEGFP (a to c), pEGFP-Cdc42 N17 (d to f), or pEGFP-RhoA N19 (g to i). After 24 h, the cells were fixed and processed for immunofluorescence, using a specific anti-*C. burnetii* antibody (red) (b, e, and h). Cells were analyzed by confocal microscopy. Micrographs of representative cells are shown. PVs are indicated by arrows. The colocalization is shown in the merge column (c, f, and i). Bars, 5 μm. (B) Quantification of colocalization. Results are means ± SE for at least three independent experiments. (C) Overexpression of the dominant-negative mutant EFGP-RhoA N19 reduces PV size. Cells were treated and processed as described for panel A. The sizes of the vacuoles were determined by morphometric analysis (see Materials and Methods). Results are expressed as means ± SE for at least three independent experiments. ***, $P < 0.001$.

shown). These results suggest that the cargo and lysosomal characteristics of the vacuoles were not affected by overexpression of the RhoA N19 mutant.

DISCUSSION

C. burnetii is a particular obligate intracellular pathogen that survives and replicates in an acidic PV with lysosomal (1, 25, 27, 64) and autophagolysosomal (7, 24, 55) features. In this report, we have shown that F-actin forms patches around the PV membrane and, more importantly, that the formation of stereotypical PVs is dependent on F-actin, as large vacuoles were not formed in infected cells treated with the actin-depolymerizing agents latrunculin B and cytochalasin D. This treatment apparently did not affect *C. burnetii* intracellular viability, as the large and spacious vacuoles harboring *C. burnetii* developed 24 h after drug washout. It is known that latrunculin B disassembles actin filaments by sequestering actin monomers, while cytochalasin D binds to the barbed end of the filaments. We observed a stronger effect with latrunculin B than with cytochalasin D. Given latrunculin's mechanism of action, our results suggest that de novo formation of F-actin is needed for the biogenesis of the large PV.

It has been shown that F-actin assembles on phagosomes containing latex beads and that this event is involved in the aggregation and tethering of phagosomes, endosomes, and lysosomes prior to membrane fusion (14, 33, 60). The interaction between phagosomes and endocytic compartments and the role of the

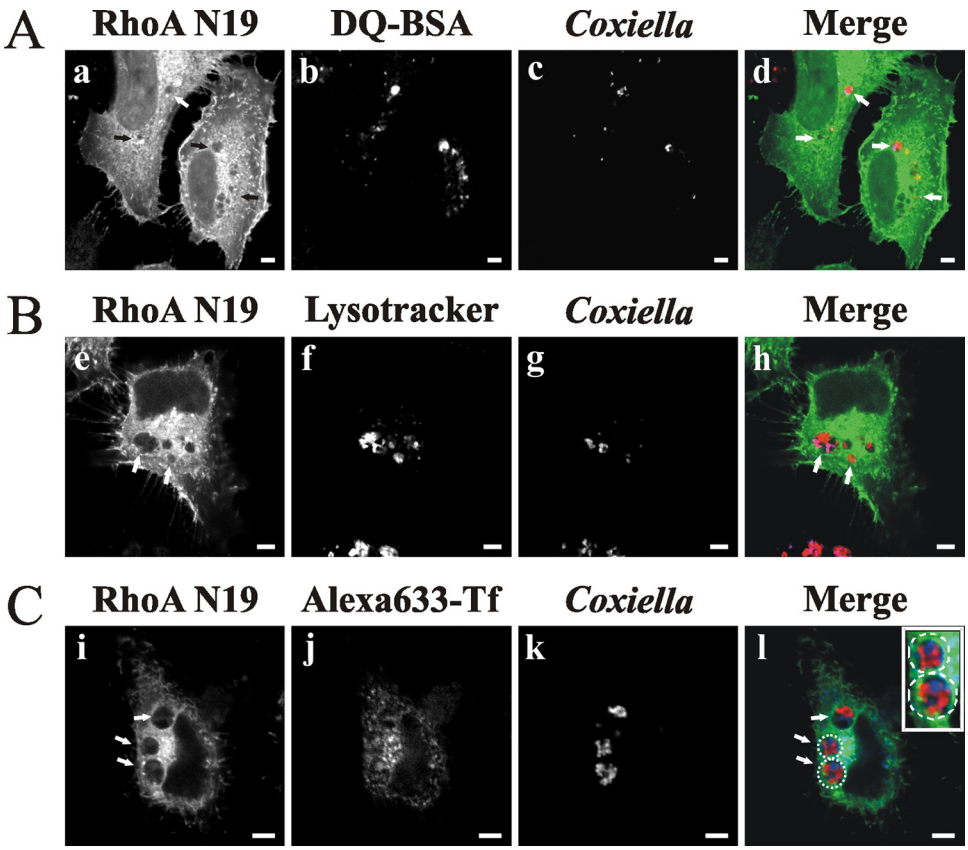

FIG. 7. Overexpression of the dominant-negative mutant of RhoA does not modify the cargo and lysosomal characteristics of PVs. Infected HeLa cells were transfected with pEGFP-RhoA N19 (a, e, and i). After 24 h, the cells were incubated (see Materials and Methods) with either DQ-BSA (A, panel b) (red), Lysotracker (B, panel f) (red), or transferrin (C, panel j) (blue). Cells were fixed and processed for immunofluorescence, using a specific anti-*C. burnetii* antibody (blue [c and g] or red [k]). Cells were analyzed by confocal microscopy. Micrographs of representative cells are shown. PVs are indicated by arrows. The colocalization between PV, expressed proteins, and markers is shown in the merge column (d, h, and l). The inset in panel l shows the localization of transferrin (blue) in the delineated vacuoles harboring the bacteria (red). Bars, 5 μm.

actin cytoskeleton have been reproduced and characterized in an "in vitro" system (17, 36, 60). Basically, the F-actin assembled on phagosomes may represent "tracks" by which late endosomes and/or lysosomes travel toward phagosomes to facilitate fusion between these compartments. In cells treated with F-actin-depolymerizing agents, a significant inhibition of fusion between latex bead-containing phagosomes and endocytic compartments was observed (14, 33, 60). It is known that the PV can be loaded with fluid-phase endocytic markers and that it is highly fusogenic and interacts with phago-endocytic compartments. Consistent with the observations described above, we observed an inhibition of the arrival of phagocytosed latex beads at the PV in cells treated with latrunculin. At early times after infection, small phagosomes containing bacteria fuse with each other to generate larger compartments (20, 25, 28, 63). Since we observed that actin depolymerization markedly reduced PV size, our results suggest that F-actin is involved not only in heterotypic fusion of PVs with latex bead-containing phagosomes but also in homotypic fusion among small PVs. The presence of F-actin on PVs and the effect of actin-depolymerizing agents indicate that F-actin likely plays a role in membrane transport events needed to form the typical PV. As mentioned before, the PV is highly fusogenic, and it is possible that different sources of membrane are needed for its formation. While our results show that endocytic and lysosomal compartments interact with the PV in latrunculin-treated cells, the small size of the PVs suggests that latrunculin inhibits the membrane contributions from other intracellular compartments.

Actin dynamics are regulated mainly by GTPases of the Rho family (53). Although several actin-related proteins have been found on latex bead-containing phagosomes, including Cdc42, this protein does not seem to play a role in actin assembly on phagosomes (13, 14, 19). However, in our system, both the WT forms and the constitutively active mutants of Cdc42 and RhoA were recruited to the PV membrane, suggesting the participation of these proteins in vacuole formation. Interestingly, the most dramatic vacuole size changes were observed in cells expressing the dominant-negative RhoA N19 mutant. The expression of this RhoA mutant inhibited the formation of large vacuoles without affecting their interaction with endocytic compartments (i.e., we still observed transferrin and Lysotracker accumulation and DQ-BSA degradation). Unfortunately, we were unable to detect internalized latex beads in *Coxiella*-infected HeLa cells overexpressing EGFP-RhoA N19, so we could not determine if overexpression of this dominant-negative mutant inhibits the fusion of the PV with latex bead phagosomes, as latrunculin does. It is likely that overexpression of

this mutant impedes bead uptake (i.e., phagocytosis). One possible solution to this problem would be to use another cell type with much higher phagocytic activity than that of HeLa cells, such as macrophages. Experiments are under way in our laboratory to determine the role of Rho proteins in latex beads and *C. burnetii* internalization. In any case, our results suggest that RhoA is required for vesicle transport and/or fusion of the *C. burnetii*-containing vacuole with other intracellular compartments. Recently, it was shown that latrunculin inhibits post-Golgi transport (39) and that Rho proteins and actin are involved in the regulation of the exocytic pathway (11, 18, 44). It is known that different sorting signals and tubular-vesicular compartments participate in the biosynthetic route (54). It would be interesting to use our system to study whether F-actin and Rho proteins have a role in the recruitment of specific subsets of secretory vesicles to promote their selective fusion with the PV during the intracellular trafficking of *C. burnetii*.

The inhibition of PV formation (29) and the significant decrease of WT RhoA colocalization with the PV (our results) in cells treated with chloramphenicol suggest an important role for bacterial protein synthesis in the connection between PV formation and Rho proteins. *Legionella pneumophila* and *C. burnetii* were shown to contain an *icm*/*dot* type IVB secretion system (57, 67). It has been shown that this system is required for the vacuole formation and successful intracellular growth of *L. pneumophila* (31, 58). The *icm*/*dot* secretion system translocates effectors into host cells to interact with and modulate the activity of host proteins known to regulate the secretory pathway, such as Arf1 (49), Rab1 (8, 30, 43), and Sec22b (16, 34). Interestingly, overexpression of Rab1 in *C. burnetii*-infected cells regulates PV formation (E. Campoy and M. Colombo, unpublished data), suggesting a relationship between the secretory pathway and PV formation. Because some of these bacterial effectors have guanine nucleotide exchange factor and GAP activities, it is likely that *C. burnetii* effectors secreted by the type IV secretion system exhibit similar activities on Rho GTPases. This is in concordance with the inhibition of Rho protein recruitment to PVs when bacterial protein synthesis was stopped by chloramphenicol treatment of infected cells. Genetic manipulations of *C. burnetii* are hard to perform. However, as reported in a very recent publication, the first mutant has been generated (6). Advances in that area will allow testing of our hypothesis in the future.

It has been shown that phagosomes containing nonpathogenic or killed pathogenic mycobacteria are able to recruit F-actin but that those that contain live pathogenic bacteria are not (2, 3, 23). Actin nucleation, in a way that is not completely understood, correlates with the fusion of phagosomes with late endocytic-lysosomal compartments, an event that favors the killing of bacteria. On the other hand, it has been observed that phagosomes harboring *Leishmania* accumulate actin in a Cdc42- and Rac1-dependent manner and that this periphagosomal actin coat is involved in delaying the maturation of the phagosomes (40, 42). In our experiments, the accumulation of Lysotracker, a marker that labels acidic (pH 5) and mature endosome compartments, and the degradation of DQ-BSA in the PV suggest that overexpression of RhoA N19 and Cdc42 (data not shown) did not significantly affect endocytic trafficking during the PV formation process.

Recently, it was shown that not only is F-actin recruited to the *Chlamydia trachomatis* vacuole in a RhoA-dependent manner but these proteins also act to maintain the morphology and integrity of the vacuole (37). Surprisingly, WT RhoA and its constitutively active and dominant-negative mutants are recruited equally to the *C. trachomatis* vacuole. Our results show that both the WT and the constitutively active RhoA mutant, but not the dominant-negative RhoA mutant, are recruited to PV-containing *C. burnetii*, suggesting that the nucleotide-bound state of RhoA is important. Notably, the expression of the dominant-negative mutant of RhoA modified the size of the vacuole without affecting its integrity.

The interaction of the PV with F-actin and its role in the biogenesis of the typical *C. burnetii* vacuole, together with results from other laboratories, establish the relationship between pathogen-containing phagosomes and the actin cytoskeleton. Our results also support the participation of actin in the motility and fusion of endosomes, lysosomes, and phagosomes. How actin and Rho proteins are recruited to the PV membrane and how these proteins are involved in the formation of this vacuole are currently under investigation in our laboratory.

ACKNOWLEDGMENTS

We thank Philippe Chavrier and Mark R. Phillips for their generous gifts of plasmids encoding Rho proteins and their mutants, Robert Heinzen for its generous gift of rabbit polyclonal anti-*Coxiella* antibody, and Ted Hackstadt for providing *C. burnetii*. We also thank Luis Mayorga for a critical reading of the manuscript.

This work was supported by grants from CONICET (PIP 5794), Agencia Nacional de Promoción Científica y Tecnológica (PICT2005 no. 38077), and SECTyP-Universidad Nacional de Cuyo (06/J108) to W.B.

REFERENCES

1. **Akporiaye, E. T., J. D. Rowatt, A. A. Aragon, and O. G. Baca.** 1983. Lysosomal response of a murine macrophage-like cell line persistently infected with *Coxiella burnetii*. Infect. Immun. **40:**1155–1162.
2. **Anes, E., M. P. Kuhnel, E. Bos, J. Moniz-Pereira, A. Habermann, and G. Griffiths.** 2003. Selected lipids activate phagosome actin assembly and maturation resulting in killing of pathogenic mycobacteria. Nat. Cell Biol. **5:**793–802.
3. **Anes, E., P. Peyron, L. Staali, L. Jordao, M. G. Gutierrez, H. Kress, M. Hagedorn, I. Maridonneau-Parini, M. A. Skinner, A. G. Wildeman, S. A. Kalamidas, M. Kuehnel, and G. Griffiths.** 2006. Dynamic life and death interactions between *Mycobacterium smegmatis* and J774 macrophages. Cell. Microbiol. **8:**939–960.
4. **Aspenstrom, P., A. Fransson, and J. Saras.** 2004. Rho GTPases have diverse effects on the organization of the actin filament system. Biochem. J. **377:** 327–337.
5. **Baca, O. G., and D. Paretsky.** 1983. Q fever and *Coxiella burnetii*: a model for host-parasite interactions. Microbiol. Rev. **47:**127–149.
6. **Beare, P. A., D. Howe, D. C. Cockrell, A. Omsland, B. Hansen, and R. A. Heinzen.** 2008. Characterization of a *Coxiella burnetii ftsZ* mutant generated by Himar1 transposon mutagenesis. J. Bacteriol. **191:**1369–1381.
7. **Beron, W., M. G. Gutierrez, M. Rabinovitch, and M. I. Colombo.** 2002. *Coxiella burnetii* localizes in a Rab7-labeled compartment with autophagic characteristics. Infect. Immun. **70:**5816–5821.
8. **Brombacher, E., S. Urwyler, C. Ragaz, S. S. Weber, K. Kami, M. Overduin, and H. Hilbi.** 2009. Rab1 guanine nucleotide exchange factor SidM is a major phosphatidylinositol 4-phosphate-binding effector protein of *Legionella pneumophila*. J. Biol. Chem. **284:**4846–4856.
9. **Bustelo, X. R., V. Sauzeau, and I. M. Berenjeno.** 2007. GTP-binding proteins of the Rho/Rac family: regulation, effectors and functions in vivo. Bioessays **29:**356–370.
10. **Caron, E., and A. Hall.** 1998. Identification of two distinct mechanisms of phagocytosis controlled by different Rho GTPases. Science **282:**1717–1721.
11. **Chen, J. L., L. Lacomis, H. Erdjument-Bromage, P. Tempst, and M. Stamnes.** 2004. Cytosol-derived proteins are sufficient for Arp2/3 recruitment and ARF/coatomer-dependent actin polymerization on Golgi membranes. FEBS Lett. **566:**281–286.
12. Reference deleted.
13. **Defacque, H., E. Bos, B. Garvalov, C. Barret, C. Roy, P. Mangeat, H. W. Shin, V. Rybin, and G. Griffiths.** 2002. Phosphoinositides regulate membrane-dependent actin assembly by latex bead phagosomes. Mol. Biol. Cell **13:**1190–1202.

14. **Defacque, H., M. Egeberg, A. Habermann, M. Diakonova, C. Roy, P. Mangeat, W. Voelter, G. Marriott, J. Pfannstiel, H. Faulstich, and G. Griffiths.** 2000. Involvement of ezrin/moesin in de novo actin assembly on phagosomal membranes. EMBO J. **19:**199–212.
15. **DeMali, K. A., and K. Burridge.** 2003. Coupling membrane protrusion and cell adhesion. J. Cell Sci. **116:**2389–2397.
16. **Derre, I., and R. R. Isberg.** 2004. *Legionella pneumophila* replication vacuole formation involves rapid recruitment of proteins of the early secretory system. Infect. Immun. **72:**3048–3053.
17. **Desjardins, M., and G. Griffiths.** 2003. Phagocytosis: latex leads the way. Curr. Opin. Cell Biol. **15:**498–503.
18. **Dubois, T., O. Paleotti, A. A. Mironov, V. Fraisier, T. E. Stradal, M. A. De Matteis, M. Franco, and P. Chavrier.** 2005. Golgi-localized GAP for Cdc42 functions downstream of ARF1 to control Arp2/3 complex and F-actin dynamics. Nat. Cell Biol. **7:**353–364.
19. **Garin, J., R. Diez, S. Kieffer, J. F. Dermine, S. Duclos, E. Gagnon, R. Sadoul, C. Rondeau, and M. Desjardins.** 2001. The phagosome proteome: insight into phagosome functions. J. Cell Biol. **152:**165–180.
20. **Gomes, M. S., S. Paul, A. L. Moreira, R. Appelberg, M. Rabinovitch, and G. Kaplan.** 1999. Survival of *Mycobacterium avium* and *Mycobacterium tuberculosis* in acidified vacuoles of murine macrophages. Infect. Immun. **67:**3199–3206.
21. **Gourlay, C. W., and K. R. Ayscough.** 2005. A role for actin in aging and apoptosis. Biochem. Soc. Trans. **33:**1260–1264.
22. **Guerin, I., and C. de Chastellier.** 2000. Pathogenic mycobacteria disrupt the macrophage actin filament network. Infect. Immun. **68:**2655–2662.
23. **Guerin, I., and C. de Chastellier.** 2000. Disruption of the actin filament network affects delivery of endocytic contents marker to phagosomes with early endosome characteristics: the case of phagosomes with pathogenic mycobacteria. Eur. J. Cell Biol. **79:**735–749.
24. **Gutierrez, M. G., C. L. Vazquez, D. B. Munafo, F. C. Zoppino, W. Beron, M. Rabinovitch, and M. I. Colombo.** 2005. Autophagy induction favours the generation and maturation of the *Coxiella*-replicative vacuoles. Cell. Microbiol. **7:**981–993.
25. **Heinzen, R. A., M. A. Scidmore, D. D. Rockey, and T. Hackstadt.** 1996. Differential interaction with endocytic and exocytic pathways distinguish parasitophorous vacuoles of *Coxiella burnetii* and *Chlamydia trachomatis*. Infect. Immun. **64:**796–809.
26. **Henry, R. M., A. D. Hoppe, N. Joshi, and J. A. Swanson.** 2004. The uniformity of phagosome maturation in macrophages. J. Cell Biol. **164:**185–194.
27. **Howe, D., and L. P. Mallavia.** 2000. *Coxiella burnetii* exhibits morphological change and delays phagolysosomal fusion after internalization by J774A.1 cells. Infect. Immun. **68:**3815–3821.
28. **Howe, D., J. Melnicakova, I. Barak, and R. A. Heinzen.** 2003. Fusogenicity of the *Coxiella burnetii* parasitophorous vacuole. Ann. N. Y. Acad. Sci. **990:** 556–562.
29. **Howe, D., J. Melnicakova, I. Barak, and R. A. Heinzen.** 2003. Maturation of the *Coxiella burnetii* parasitophorous vacuole requires bacterial protein synthesis but not replication. Cell. Microbiol. **5:**469–480.
30. **Ingmundson, A., A. Delprato, D. G. Lambright, and C. R. Roy.** 2007. *Legionella pneumophila* proteins that regulate Rab1 membrane cycling. Nature **450:**365–369.
31. **Isberg, R. R., T. J. O'Connor, and M. Heidtman.** 2009. The *Legionella pneumophila* replication vacuole: making a cosy niche inside host cells. Nat. Rev. Microbiol. **7:**13–24.
32. **Jaffe, A. B., and A. Hall.** 2005. Rho GTPases: biochemistry and biology. Annu. Rev. Cell Dev. Biol. **21:**247–269.
33. **Jahraus, A., M. Egeberg, B. Hinner, A. Habermann, E. Sackman, A. Pralle, H. Faulstich, V. Rybin, H. Defacque, and G. Griffiths.** 2001. ATP-dependent membrane assembly of F-actin facilitates membrane fusion. Mol. Biol. Cell **12:**155–170.
34. **Kagan, J. C., M. P. Stein, M. Pypaert, and C. R. Roy.** 2004. *Legionella* subvert the functions of Rab1 and Sec22b to create a replicative organelle. J. Exp. Med. **199:**1201–1211.
35. **Kaksonen, M., C. P. Toret, and D. G. Drubin.** 2006. Harnessing actin dynamics for clathrin-mediated endocytosis. Nat. Rev. Mol. Cell Biol. **7:**404–414.
36. **Kjeken, R., M. Egeberg, A. Habermann, M. Kuehnel, P. Peyron, M. Floetenmeyer, P. Walther, A. Jahraus, H. Defacque, S. A. Kuznetsov, and G. Griffiths.** 2004. Fusion between phagosomes, early and late endosomes: a role for actin in fusion between late, but not early endocytic organelles. Mol. Biol. Cell **15:**345–358.
37. **Kumar, Y., and R. H. Valdivia.** 2008. Actin and intermediate filaments stabilize the *Chlamydia trachomatis* vacuole by forming dynamic structural scaffolds. Cell Host Microbe **4:**159–169.
38. **Ladwein, M., and K. Rottner.** 2008. On the Rho'd: the regulation of membrane protrusions by Rho-GTPases. FEBS Lett. **582:**2066–2074.
39. **Lazaro-Dieguez, F., C. Colonna, M. Cortegano, M. Calvo, S. E. Martinez, and G. Egea.** 2007. Variable actin dynamics requirement for the exit of different cargo from the trans-Golgi network. FEBS Lett. **581:**3875–3881.
40. **Lerm, M., A. Holm, A. Seiron, E. Sarndahl, K. E. Magnusson, and B. Rasmusson.** 2006. *Leishmania donovani* requires functional Cdc42 and Rac1 to prevent phagosomal maturation. Infect. Immun. **74:**2613–2618.
41. **Li, S., J. L. Guan, and S. Chien.** 2005. Biochemistry and biomechanics of cell motility. Annu. Rev. Biomed. Eng. **7:**105–150.
42. **Lodge, R., and A. Descoteaux.** 2005. *Leishmania donovani* promastigotes induce periphagosomal F-actin accumulation through retention of the GTPase Cdc42. Cell. Microbiol. **7:**1647–1658.
43. **Machner, M. P., and R. R. Isberg.** 2007. A bifunctional bacterial protein links GDI displacement to Rab1 activation. Science **318:**974–977.
44. **Matas, O. B., S. Fritz, A. Luna, and G. Egea.** 2005. Membrane trafficking at the ER/Golgi interface: functional implications of RhoA and Rac1. Eur. J. Cell Biol. **84:**699–707.
45. **May, R. C., and L. M. Machesky.** 2001. Phagocytosis and the actin cytoskeleton. J. Cell Sci. **114:**1061–1077.
46. Reference deleted.
47. **Merrifield, C. J., D. Perrais, and D. Zenisek.** 2005. Coupling between clathrin-coated-pit invagination, cortactin recruitment, and membrane scission observed in live cells. Cell **121:**593–606.
48. Reference deleted.
49. **Nagai, H., J. C. Kagan, X. Zhu, R. A. Kahn, and C. R. Roy.** 2002. A bacterial guanine nucleotide exchange factor activates ARF on *Legionella* phagosomes. Science **295:**679–682.
50. **Niedergang, F., and P. Chavrier.** 2005. Regulation of phagocytosis by Rho GTPases. Curr. Top. Microbiol. Immunol. **291:**43–60.
51. **Qualmann, B., and H. Mellor.** 2003. Regulation of endocytic traffic by Rho GTPases. Biochem. J. **371:**233–241.
52. **Rabinovitch, M.** 1995. Professional and non-professional phagocytes: an introduction. Trends Cell Biol. **5:**85–87.
53. **Ridley, A. J.** 2006. Rho GTPases and actin dynamics in membrane protrusions and vesicle trafficking. Trends Cell Biol. **16:**522–529.
54. **Rodriguez-Boulan, E., and A. Musch.** 2005. Protein sorting in the Golgi complex: shifting paradigms. Biochim. Biophys. Acta **1744:**455–464.
55. **Romano, P. S., M. G. Gutierrez, W. Beron, M. Rabinovitch, and M. I. Colombo.** 2007. The autophagic pathway is actively modulated by phase II *Coxiella burnetii* to efficiently replicate in the host cell. Cell. Microbiol. **9:**891–909.
56. **Scott, C. C., W. Dobson, R. J. Botelho, N. Coady-Osberg, P. Chavrier, D. A. Knecht, C. Heath, P. Stahl, and S. Grinstein.** 2005. Phosphatidylinositol-4,5-bisphosphate hydrolysis directs actin remodeling during phagocytosis. J. Cell Biol. **169:**139–149.
57. **Segal, G., M. Feldman, and T. Zusman.** 2005. The Icm/Dot type-IV secretion systems of *Legionella pneumophila* and *Coxiella burnetii*. FEMS Microbiol. Rev. **29:**65–81.
58. **Shin, S., and C. R. Roy.** 2008. Host cell processes that influence the intracellular survival of *Legionella pneumophila*. Cell. Microbiol. **10:**1209–1220.
59. **Stamnes, M.** 2002. Regulating the actin cytoskeleton during vesicular transport. Curr. Opin. Cell Biol. **14:**428–433.
60. **Stockinger, W., S. C. Zhang, V. Trivedi, L. A. Jarzylo, E. C. Shieh, W. S. Lane, A. B. Castoreno, and A. Nohturfft.** 2006. Differential requirements for actin polymerization, calmodulin, and Ca2+ define distinct stages of lysosome/phagosome targeting. Mol. Biol. Cell **17:**1697–1710.
61. **Swanson, J. A., M. T. Johnson, K. Beningo, P. Post, M. Mooseker, and N. Araki.** 1999. A contractile activity that closes phagosomes in macrophages. J. Cell Sci. **112:**307–316.
62. **Unsworth, K. E., M. Way, M. McNiven, L. Machesky, and D. W. Holden.** 2004. Analysis of the mechanisms of *Salmonella*-induced actin assembly during invasion of host cells and intracellular replication. Cell. Microbiol. **6:**1041–1055.
63. **Veras, P. S., C. de Chastellier, M. F. Moreau, V. Villiers, M. Thibon, D. Mattei, and M. Rabinovitch.** 1994. Fusion between large phagocytic vesicles: targeting of yeast and other particulates to phagolysosomes that shelter the bacterium *Coxiella burnetii* or the protozoan *Leishmania amazonensis* in Chinese hamster ovary cells. J. Cell Sci. **107:**3065–3076.
64. **Voth, D. E., and R. A. Heinzen.** 2007. Lounging in a lysosome: the intracellular lifestyle of *Coxiella burnetii*. Cell. Microbiol. **9:**829–840.
65. **Woldehiwet, Z.** 2004. Q fever (coxiellosis): epidemiology and pathogenesis. Res. Vet. Sci. **77:**93–100.
66. **Yates, R. M., A. Hermetter, and D. G. Russell.** 2005. The kinetics of phagosome maturation as a function of phagosome/lysosome fusion and acquisition of hydrolytic activity. Traffic **6:**413–420.
67. **Zamboni, D. S., S. McGrath, M. Rabinovitch, and C. R. Roy.** 2003. *Coxiella burnetii* express type IV secretion system proteins that function similarly to components of the Legionella pneumophila Dot/Icm system. Mol. Microbiol. **49:**965–976.
68. **Zhang, F., F. S. Southwick, and D. L. Purich.** 2002. Actin-based phagosome motility. Cell Motil. Cytoskelet. **53:**81–88.

Editor: R. P. Morrison